Analytica Chimica Acta 1221 (2022) 340134

Contents lists available at ScienceDirect

Analytica Chimica Acta

journal homepage: www.elsevier.com/locate/aca

A molecular beacon biosensor for viral RNA detection based on HyCaSD strategy

W. Saisuk [a], C. Srisawat [c,e], S. Yoksan [d], T. Dharakul [b,e,*]

[a] Department of Research, Faculty of Medicine Siriraj Hospital, Mahidol University, Bangkok, 10700, Thailand
[b] Department of Immunology, and, Faculty of Medicine Siriraj Hospital, Mahidol University, Bangkok, 10700, Thailand
[c] Department of Biochemistry, Faculty of Medicine Siriraj Hospital, Mahidol University, Bangkok, 10700, Thailand
[d] Institute of Molecular Biosciences, Mahidol University, Nakhon Pathom, 73170, Thailand
[e] Research Network NANOTEC, MU in Theranostic Nanomedicine, Thailand

HIGHLIGHTS

- Hybridization Cascade plus Strand-Displacement Amplification (HyCaSD) and molecular beacon for viral RNA detection.
- Excellent sensitivity and selectivity of the viral RNA detection method.
- A single-step, single-tube and actual-time RNA detection procedure.

GRAPHICAL ABSTRACT

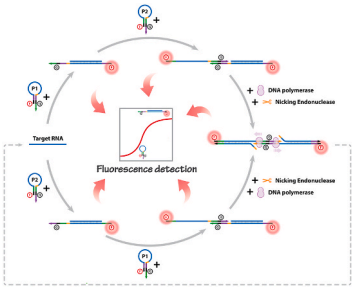

ARTICLE INFO

Keywords:
Isothermal amplification
Molecular beacon biosensor
Dengue virus
RNA secondary Structure

ABSTRACT

In the present study, a molecular beacon biosensor was developed to enable efficient detection of the viral RNAs using a previously described HyCaSD platform. The HyCaSD molecular beacon probes were labeled with the Cy5 and BHQ3 at each end of the hairpin probes. The fluorescent signal was detected immediately only when the molecular beacon probes specifically hybridized to the target sequence and unfolded their hairpin structures. This combination greatly improved the sensitivity with LOD of 100 copy equivalents per reaction (around 20-fold greater than the original HyCaSD). In addition, our MB-based HyCaSD demonstrated a single-step, single-tube and actual-time RNA detection procedure, thereby bringing it a major step closer to point-of-care diagnostic applications for viral infectious diseases.

1. Introduction

Molecular beacon biosensors are attractive due to their ability to merge excellent sensitivity and selectivity for biological target detection. The molecular beacon probes are easily designed and synthesized, and can practically recognize any DNA and RNA target of interest. In addition, the molecular beacon technology possesses important features such as simplicity and rapid generation of results,

* Corresponding author. Department of Immunology, Faculty of Medicine Siriraj Hospital, Mahidol University. 2 WangLang Road, Bangkok Noi, Bangkok, 10700, Thailand.
E-mail address: tararaj.dha@mahidol.ac.th (T. Dharakul).

https://doi.org/10.1016/j.aca.2022.340134
Received 2 June 2022; Accepted 26 June 2022
Available online 1 July 2022

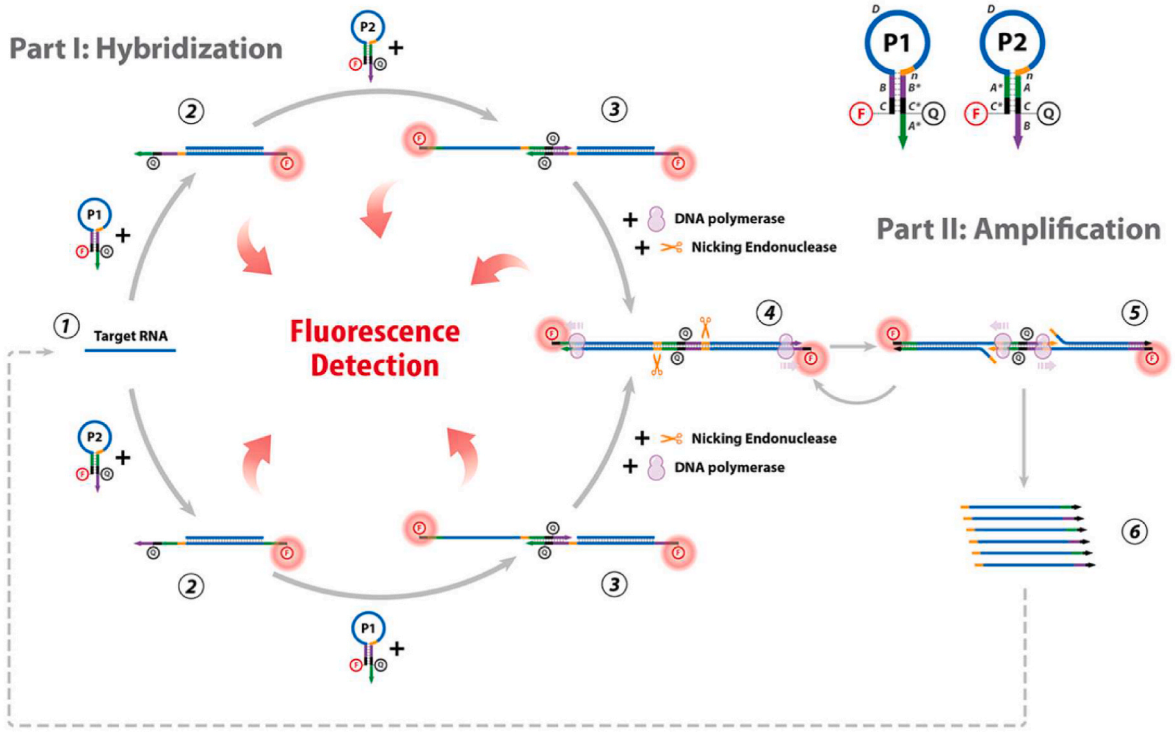

Scheme 1. Molecular beacon-based Hybridization Cascade plus Strand-Displacement Amplification (MB-based HyCaSD). The scheme for target RNA detection with MB-based HyCaSD is shown in sequential steps, composed of the hybridization (step 1, 2 and 3) followed by the amplification part (step 4 and 5). The P1 or P2 probe alone maintained their hairpin structure with the fluorophore and the quencher stayed close to each other, resulting in strong quenching of the fluorescence signal. Part I Probe hybridization step: in the presence of the RNA target, target sequence (in blue) was hybridized by the loop (domain D) of either the P1 or P2 probe. The hybridization unfolded the probe's stem structure into an opened, single-stranded structure (domains B* C* A* or A C B). The fluorophore and its quencher were thus separated and immediately emitted the fluorescence signal. The first unfolded probe allowed the second probe to hybridize using its toehold sequence (domain A* or B), initiating the strand-displacement mechanism to form a P1–P2 probe complex while also emitting the fluorescence signal. After probe hybridization, the Bst 2.0 DNA polymerase extended the DNA strands in 2 directions, generating a dsDNA complex with a nicking endonuclease recognition site on both strands. Part II DNA amplification step: the complex was nicked by Nb.BsmI nicking endonuclease, initiating strand-displacement amplification on both strands of the dsDNA complex at once. The released ssDNA became a new target for another round of probe hybridization.

which are fully suitable for point-of-care (POC) application. Therefore, molecular beacon-based biosensors have been widely used to integrate with several techniques to enable diagnostic applications, especially for infectious diseases.

Isothermal amplification is a simple and powerful DNA/RNA amplification method, which has been developed for viral RNA detection [1–11]. We recently demonstrated a highly sensitive isothermal amplification, called Hybridization Cascade plus Strand-Displacement Amplification (HyCaSD), for the detection of an RNA target [12]. The HyCaSD method showed promising selectivity and sensitivity with the limit of detection (LOD) in the femtomolar (fM; 10^{-15} M) range for the synthetic RNA targets as well as the viral RNAs. However, its limitation is a requirement of post-staining step to measure the detection signal. Post-staining with a DNA staining dye (such as ethidium bromide or SYBR Green I), is not only mutagenic and carcinogenic [13–15] but also generates the false positive signal because of their ability to bind mainly to double-stranded DNA/RNA, and SYBR Gold also binds to single-stranded sequences, including non-target sequences [16–20]. The non-specific binding leads to the reduced sensitivity and selectivity of the detection. In addition, the post staining requires additional steps and is unfavorable for real-time signal detection, an ideal feature of POC setting.

In the present study, a molecular beacon biosensor was incorporated into the HyCaSD (see Scheme 1) to further enhance the efficiency of the method in detecting viral RNAs. Based on molecular beacon probe design, a fluorescent dye and its quencher were labeled at each end of the HyCaSD hairpin probes. Thus, the fluorescent signal was detected immediately only when the DNA probes specifically hybridized to the target sequence and unfolded their hairpin structures, with no requirement of post-staining. Compared to the original HyCaSD, the molecular beacon-based HyCaSD (MB-based HyCaSD) successfully improved the sensitivity for detection of the synthetic targets as well as the viral RNAs, which greatly enhanced the LOD from fM to attomolar (aM; 10^{-18} M) range. In addition to improvement of the detection efficiency, this

Table 1
Sequences of the synthetic target, primers, and DNA probes. The italic sequence represents an additional T7 promoter sequence, the wave underlined sequence represents the probe binding site, the bold sequence represents the stem structure of the probes, and the underlined sequence represents the nicking endonuclease recognition sequence. The (F) and the (Q) represent the labeled fluorophore and the labeled quencher, respectively.

Definition	Sequence
105-nt synthetic target	AGCATATTGACGCTGGGAAAGACCAGAGATCCTGCTGTCTCTAC AGCATCATTCCAGGCACAGAACGCCAGAAAATGGAATGGTGCT GTTGAATCAACAGGTTCT
26-nt synthetic target	CATATTGACGCTGGGAAAGACCAGAG
24-nt non-target	ATGGTGGGTAATACTGTATAATCC
T7-forward primer	*TAATACGACTCACTAT*AGCATATTGACGCTG
Reverse primer	AGAACCTGTTGATTC
P1 probe	**C-(F)GGGTGAGCG**GATCTCTGGTCTTTCCCAGCGTCAA GAATGCC**CGCTCACCG-(Q)**CTCCCT
P2 probe	**C-(F)CCGCTCCCT**GATCTCTGGTCTTTCCCAGCGTCAA GAATGCC**AGGGAGCGG-(Q)**TGAGCG

combination enabled a single-step, single-tube detection platform, and exhibited an actual-time RNA detection. This was a major step closer to POC diagnostic applications for viral infectious diseases.

2. Materials and methods

2.1. Materials

The probes were simulated and designed using NUPACK web-based software (http://www.nupack.org/) [21]. The Cy5 fluorescent dye was labeled at the 5′ end of the DNA probes, and the BHQ3 quencher was labeled at the 7th nucleotide position from the 3′ end. The labeled probes were synthesized by Bio Basic Inc. (Markham, Ontario, Canada). A DNA sequence of 105-nt in the 3′-untranslated region (UTR) of the DENV genome was synthesized and purified by Integrated DNA Technologies (Coralville, IA, USA). The primers for the *in vitro* transcription were synthesized by Bio Basic Inc. (Markham, Ontario, Canada). The detailed sequence information of the DNA and RNA used in this study is listed in Table 1. The nicking endonuclease Nb.BsmI, NEBuffer 3.1, Bst 2.0 DNA polymerase, and ThermoPol Reaction buffer were purchased from New England Biolabs, Inc. (Ipswich, MA, USA). The deoxynucleotide solution mixture (dNTP), PCR buffer, and Taq DNA polymerase were purchased from Geneaid (Taipei, Taiwan). SYBR Gold was purchased from Thermo Fisher Scientific, Inc. (Waltham, MA, USA). The ingredients for the *in vitro* transcription, including T7 RNA polymerase, adenosine triphosphate (ATP), guanosine triphosphate (GTP), 2′-fluoro-cytosine triphosphate (2′F-CTP), and 2′-fluoro-uracil triphosphate (2′F-UTP), were purchased from Epicentre Technologies, Corp. (Madison, WI, USA). The DNase I and RQ1 buffers were purchased from Promega, Corp. (Madison, WI, USA). A 24-nt synthetic DNA oligonucleotide (a part of 16*S* rRNA gene of *E. canis*) and a 93-nt synthetic $tRNA^{SER}$, the sequences of which are irrelevant to DENV, were used as non-target sequences. The 26-nt synthetic DNA, which contained 22 nucleotides that overlapped with the probe binding site (Table 1, Fig. S1).

The viruses used in the present study were propagated in C6/36 cell lines. DENV-1 strain 16007, DENV-2 strain 16681, DENV-3 strain 16562, DENV-4 strain 1036, Zika virus (ZIKV) ATCC VR-84 strain MR766, Japanese encephalitis virus (JEV) Beijing strain, Chikungunya virus (CHIKV) strain Ss08/363, and uninfected C6/36 cells were obtained from the Center for Vaccine Development, Institute of Science and Technology for Research and Development, Mahidol University (Nakhon Pathom, Thailand).

2.2. *105-Nt RNA target preparation by in vitro transcription*

A PCR reaction was performed to generate double-stranded DNA template for the *in vitro* transcription. The PCR reaction mixture consisted of 1X PCR buffer (15 mM Tris-HCl pH 8.75, 50 mM KCl, 2 mM MgCl2), 200 μM dNTPs, 2.5 U Taq DNA polymerase, 1 mM T7 promoter-forward primer and reverse primer, and 2 μM 105-nt DNA template from 3′-UTR of DENV genome in a total volume of 100 μL. The PCR conditions consisted of an initial denaturation at 95 °C for 3 min, followed by 35 cycles of denaturation at 95 °C for 30 s, primer annealing at 54 °C for 40 s, and elongation at 72 °C for 50 s. Then, final elongation was carried out at 72 °C for 3 min. The PCR product was purified by a QIAquick PCR purification kit (QIAGEN, Hilden, Germany) for *in vitro* transcription by T7 RNA polymerase.

To perform *in vitro* transcription, the purified PCR product was incubated with 2′F-transcription mix, 100 mM DTT, and 50U T7 RNA polymerase (Epicentre) at 37 °C for 6 h. The *in vitro* transcription reaction was then added to 2U DNase I (Promega) and 1X RQ1 buffer at 37 °C for 15 min. After the *in vitro* transcription, the reaction was purified using a QIAquick nucleotide removal kit as per the manufacturer's instructions (QIAGEN, Hilden, Germany). The RNA concentration was measured with a NanoDrop 8000 (Thermo Fisher Scientific Inc., Waltham, MA, USA), and the integrity of the transcript was analyzed using 3% agarose gel.

2.3. Viral RNA target preparation

Viral RNA was extracted from 140 μL of culture media of DENV, ZIKV, JEV, CHIKV, and uninfected C6/36 cells using a QIAmp Viral RNA Mini kit according to the manufacturer's instructions (QIAGEN, Hilden, Germany). The concentrations and integrity of the extracted RNA were analyzed using an absorbance of 260 nm by NanoDrop 8000 (Thermo Fisher Scientific Inc., Waltham, MA, USA) and mobility on agarose gel electrophoresis.

The extracted RNA of DENV1-4 was converted into cDNA at 42 °C for 1 h. The reaction comprised of 200U of M-MLV reverse transcriptase, 1X reaction buffer, 2 mM dNTP, 25U of rRnasin RNase inhibitor (Promega, Madison, WI, USA), and 0.5 μM the reverse primer. The viral RNA concentration was calculated using a standard curve. Real-time PCR was carried out in a LightCycler 480 (Roche Diagnostics, Indianapolis, IN, USA) with the known-concentration synthetic target DNA to construct a standard curve. The total volume of 20 μl reaction mixture was composed of different concentrations of cDNA, 1 μM each of the forward and reverse primers, 1X QuantiTect SYBR Green PCR Master Mix (QIAGEN, Hilden, Germany), 3.5 mM Mg2+, and nuclease-free water. The amplification reaction contained a preheat step at 95 °C for 15 min. Forty cycles of amplification step were then performed, including denaturation at 94 °C for 15 s, annealing at 54 °C for 15 s, and extension at 72 °C for 30 s, while continuously collecting the fluorescence data.

2.4. Molecular beacon-based Hybridization Cascade plus strand-displacement (HyCaSD) isothermal amplification

The probes and the target were diluted to 1 μM in MilliQ water immediately before use. The diluted probes and the diluted target were then incubated at 95 °C for 5 min and slowly cooled to room temperature for 50 min to let the probes and the target perfectly fold into their appropriate structures. The reaction mixtures for amplification reaction were prepared separately as Part A and Part B. Part A consisted of 50 nM P1 and P2 probes, and different concentrations of the target RNA. Part B consisted of 250 μM dNTPs, 1X NEBuffer 3.1 (100 mM NaCl, 50 mM Tris-HCl pH 7.9, 10 mM $MgCl_2$, and 100 μg mL-1 BSA), 1X ThermoPol Reaction buffer (20 mM Tris-HCl pH 8.8, 10 mM $[NH4]_2SO_4$, 10 mM KCl, 2 mM $MgSO_4$, and 0.1% Triton X-100), 3 U Nb.BsmI, and 5 U Bst 2.0 DNA polymerase, in MilliQ water. After mixing the Part A and B solutions in a volume of 50 μL, the reaction was incubated at 50 °C for 40 min.

2.5. Polyacrylamide gel electrophoresis analysis

Thirty microliters of the reaction products were mixed with 5 μL of gel loading dye and analyzed in 10% non-denaturing polyacrylamide gel electrophoresis (PAGE) in 1X TBE buffer (9 mM Tris-HCl, pH 7.9, 9 mM boric acid, and 0.2 mM EDTA) at 100 V constant voltage for 60 min. The gel was stained by SYBR Gold and imaged by gel documentation G-box (Syngene, Frederick, MD, USA).

2.6. Fluorescence analysis

The HyCaSD reaction was performed with the Cy5/BHQ3 labeled DNA probes as described above. Thirty microliters of the reaction products were dropped into a fluorescence plate and analyzed using a Synergy H1 hybrid multi-mode microplate reader (BioTek, Winooski, VT, USA) at a 640 nm excitation wavelength and 670 nm emission wavelength.

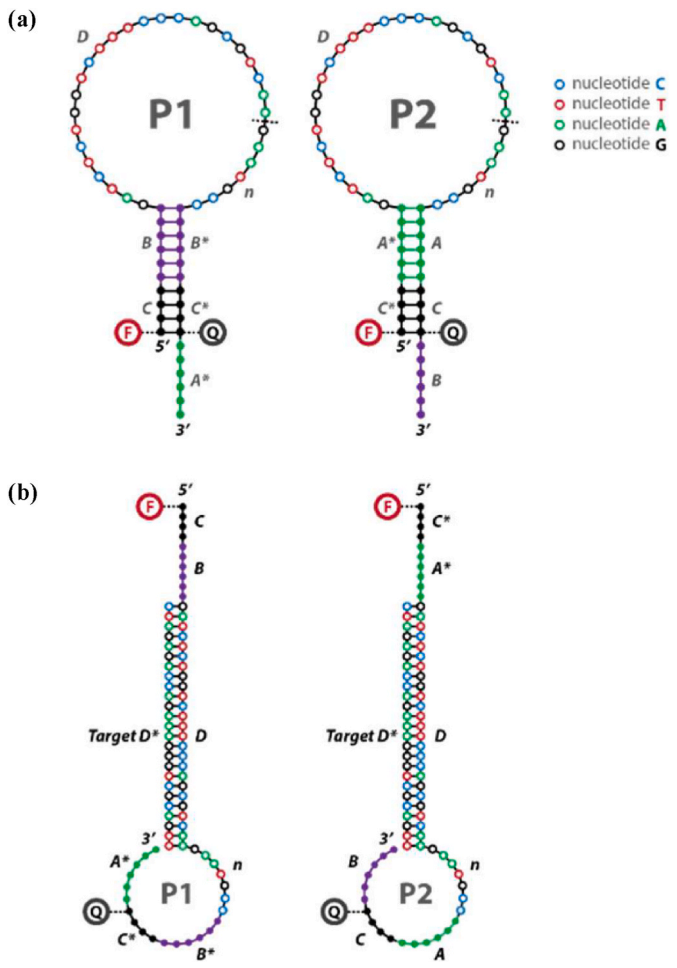

Fig. 1. P1 and P2 probe structures before **(a)** and after **(b)** target hybridization to the target. **(a)** The illustrated hairpin probes contain 3 critical parts, comprising the stem part (*C B B* C** of P1 probe and *C* A* A C* of P2 probe); the target recognition part (*D*); and the toehold part (*A** of P1 probe, and *B* of P2 probe). The nicking endonuclease recognition site was named *n*. The fluorophore (*F*) and its quencher (*Q*) were labeled at the 5′-end and at the 7th nucleotide from the 3'end of the probe, respectively. In the absence of target RNA, the probes were stably formed hairpin structures by their stem part. **(b)** In the presence of target RNA, the hairpin structure would be unfolded and hybridized to the target sequence (*D**).

3. Results and discussion

3.1. Molecular beacon probe design and principle of RNA target detection

The HyCaSD isothermal amplification has previously been demonstrated to be a promising tool to detect an RNA target even with a secondary structure [12].

In the present study, the probes were designed to enable detection of all four DENV serotypes. Due to the highly variable sequences throughout the genome among four serotypes except in 3′-UTR region, multiple sequence alignment (MSA) revealed that the conserved sequence among all four serotypes that is available for probe binding site is limited (Fig. S1). However, the 3′-UTR which was composed of approximately 450 nt, contained more than 70% of the secondary structure motifs [22].

The key component of the system is the bifunctional hairpin probes, which act as a recognition probe for target hybridization and as a template/primer for amplification. In the current study, a third functionality was added to the HyCaSD probes. Based on molecular beacon strategy, the hairpin probes were labeled with a Cy5 fluorophore at the 5′-end and with a BHQ3 quencher at the 7th nucleotide position from the 3′-end (Fig. 1a). When the probes folded into a hairpin structure, the fluorophore and the quencher molecules became closer to each other, strongly quenching the fluorescence signal. In contrast, when the hairpin probe unfolded, the fluorophore departed from the quencher and emitted the fluorescence signal (Fig. 1b). Therefore, the fluorescence signal was turned on and off, depending upon the structure of the hairpin probes. The stability of the hairpin probe structure and probe-target hybridization structure strongly depended on the designed loop and stem domains. Although the longer loop domain would enhance the efficiency of probe-target hybridization, it may give rise to a false positive signal through non-target hybridization. Conversely, the longer stem would increase stability of the hairpin probe structure, but excessive stability of the stem domain could interrupt the probe-target hybridization, leading to reduced sensitivity of the method [23–25]. Therefore, the length of the loop and stem of the hairpin probes needed to be rationally designed.

An optimal temperature (65 °C) for the chosen enzymes, Bst 2.0 DNA polymerase, and Nb.BsmI nicking endonuclease were set as a condition for the probe design using the NUPACK bioinformatic tool. The hairpin probes were designed to have a relatively larger loop domain (32 nucleotides) in order to better hybridize with the target than a typical molecular beacon probe. This strategy was based on the fact that a probe with a larger loop tended to have lower dissociation constants and higher kinetic rate constants [26–28] in order to overcome the thermodynamically unfavorable hybridization between the hairpin probe and the target [29,30]. Furthermore, the hairpin probes were rationally designed with a 10-nt stem domain, which had an adequate stability to retain the hairpin structure in the absence of the target (Fig. 1a). The hairpin probes were flexible enough to unfold when the probe hybridized to the target. Although a shorter stem is able to facilitate hybridization, it also greatly reduces the stability of the hairpin structure [31–34]. Of note, optimization of the reaction temperature that allowed the probe to retain stability of the hairpin structure and still efficiently hybridize to the target RNA was needed. A higher temperature reduced the thermodynamic stability of the stem structure, resulting in a partial opening of the hairpin probe, leading to a false-positive fluorescence signal [26,35]. Similar to the original HyCaSD, the MB-based HyCaSD consisted of the hybridization and the amplification parts (Fig. 1b). Briefly, the target sequence was recognized by the loop domain of either the P1 or P2 probe. Hybridization to the target allowed the hairpin probe to be unfolded simultaneously through the strand displacement mechanism. Upon the hairpin probe unfolding, the fluorophore and the quencher departed, and the fluorescence signal was then immediately released. The stem domain of the probe opened to a single-stranded form, provided a binding site for the toehold domain of the second probe. The toehold binding triggered strand displacement to unfold the second probe while also emitting the fluorescence signal. After hybridization, the P1 and P2 probes on the hybridization complex functioned as a primer and a template for the DNA amplification step. The DNA strands on the P1–P2 complex were extended from both 3′-ends by Bst 2.0 DNA polymerase (Fig. 1b). The double-stranded DNA, which contained recognition sites on both strands, were nicked by the Nb. BsmI endonuclease. Strand displacement amplification was then initiated by the DNA polymerase, releasing single-stranded DNA (ssDNA). The ssDNA was used as a new target for another round of probe hybridization. Every single time the probe hybridized to the target, the fluorescence signal would be released. Therefore, this fluorescence-based method allowed real-time responsive capability with no post-staining requirement by using the 3 functions of the P1 and P2 hairpin probes, including target recognition, providing a primer/template for the DNA amplification as well as fluorescence signal emission.

3.2. Verification of the molecular beacon-based HyCaSD

The HyCaSD was composed of the hybridization and the

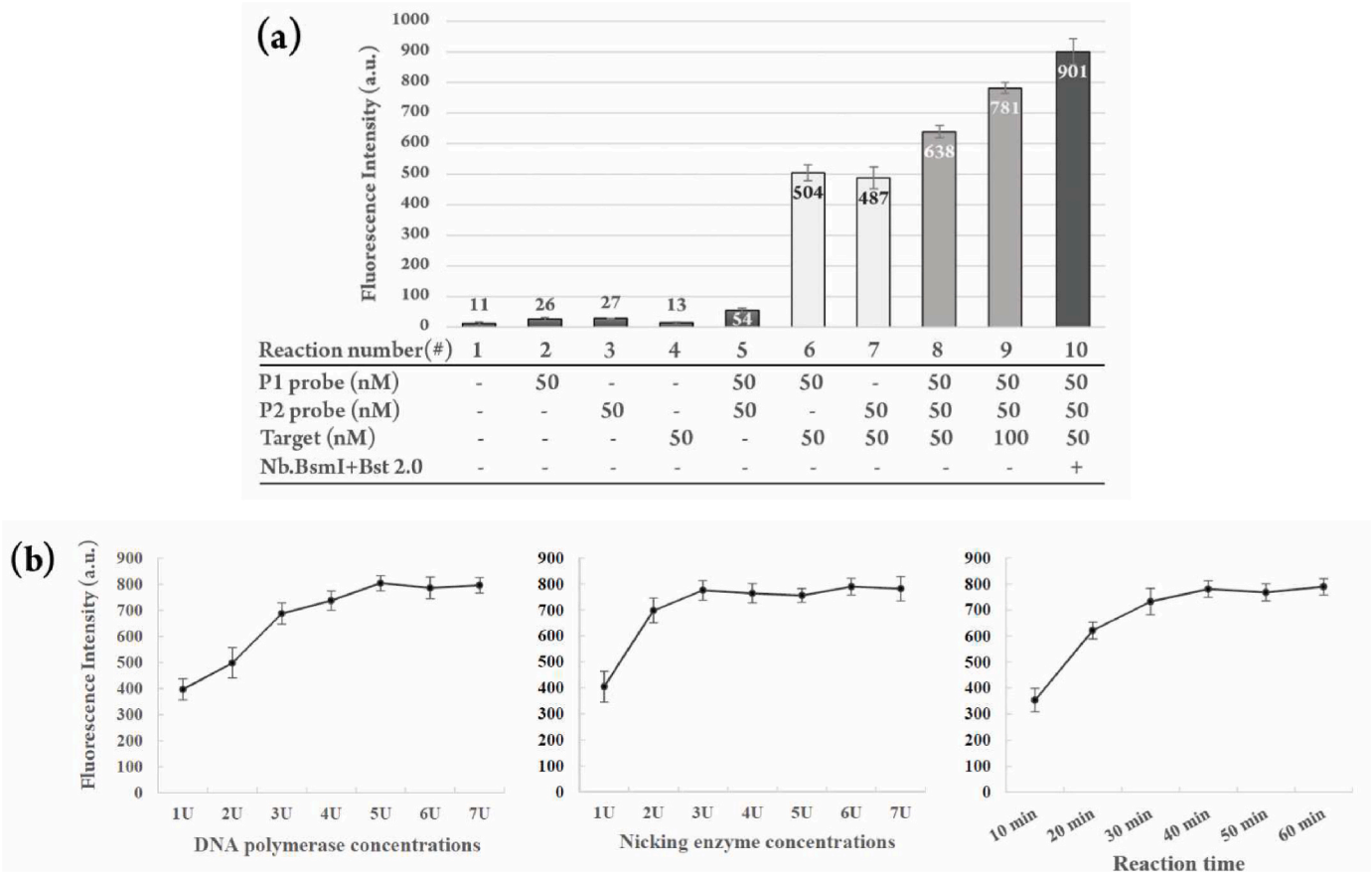

Fig. 2. Verification of the MB-based HyCaSD. **(a)** Verification of the hybridization step. The fluorescence intensity of the hybridization reaction of the MB-based HyCaSD probes with the *in vitro* transcribed 105-nt DENV RNA was monitored by fluorometer. The reactions were performed at 50 °C for 30 min. The reaction with buffer-only was set as blank. The reactions with and without P1 probe (50 nM), P2 probes (50 nM), target RNA (50 or 100 nM), and Nb.BsmI + Bst2.0 were compared. **(b)** The amplification step of the MB-based HyCaSD was verified and optimized with different concentrations of the DNA polymerase and the nicking enzyme, and various reaction times, respectively. Different concentrations of DNA polymerase were tested with fixed 5U of nicking enzyme, different concentrations of nicking enzyme were tested with fixed 5U of DNA polymerase, and the varied reaction times were optimized with 5U of DNA polymerase and 3U of nicking enzyme.

amplification parts. To verify the hybridization reaction of the P1 and P2 probes with the target, the *in vitro* transcribed 105-nt DENV RNA was used as a model target by mixing with the P1 probe and/or P2 probe. The hybridization experiments were completed within 30 min 50 °C. A significantly higher fluorescence intensity was measured from the hybridization of either the P1 or P2 probe with the target RNA (P1-Target or P2-Target) compared to the negative control (Blank, probes alone, and target alone; Fig. 2a). The slightly different fluorescence intensities of these two reactions were possibly due to a different stability level of the stem domain of the hairpin probes. The fluorescence intensity from the mixture of the P1 probe, P2 probe, and 50 nM target RNA (#8), including of four different hybridization complexes (P1-Target, P2-Target, P1–P2-Target, and Target-P1-P2-Target), was higher than those of P1-Target (#6) and P2-Target (#7) mixture, demonstrating that the second probe could subsequently hybridize to the complex after hybridization of the first probe and the target RNA. In comparison, the reactions without the target (a mixture of P1 and P2 probes) showed a very low level of fluorescence intensity from hairpin probe leakage. Whereas, the complete HyCaSD reaction with Nb.BsmI nicking endonuclease and Bst 2.0 DNA polymerase successfully amplified the template for P1 and P2 probes, resulting in the greatly increased fluorescence intensity. The results demonstrated an efficient hybridization of the designed probes to the target RNA within the study's temperature ranges. We speculated that the fluorescence intensity of the P1, P2 and target RNA mixture (#8) was less than the fluorescence intensity of each probe with the target RNA (#6, #7), due to the limited amount of the target RNA. This possibility was tested in #9 and #10 by adding more target RNA to 100 nM or adding enzymes to amplify the target RNA, respectively. The result showed increased fluorescence signal significantly, although it is not known whether the maximum fluorescence signal was achieved.

After verification of the probe hybridization, the amplification reaction was verified and optimized. The HyCaSD has been tested at varied temperatures ranging from 50 °C to 65 °C in the previous study [12]. Fifty degree Celsius was the optimal temperature for HyCaSD. The higher temperature led to false positive amplification due to thermodynamic instability of the hairpin structure of the probes and undesirable hybridization to each other. Even though 65 °C is the ideal temperature for the enzymes, they were shown to function at 50 °C. Therefore, in the present study, the temperature for MB-based HyCaSD was set at 50 °C.

The varying concentrations (1U–7U/rxn; reaction) of Bst 2.0 DNA polymerase were mixed with the P1 and P2 probes, and the 105-nt synthetic target RNA (Fig. 2b). The fluorescence intensity was increased corresponding to the higher enzyme concentration and reached a plateau at the enzyme concentration of 5U/rxn. In addition to DNA polymerase, the concentration of the Nb.BsmI nicking endonuclease was varied from 1U/rxn to 7U/rxn (Fig. 2b). Three units of nicking endonuclease were the optimal concentration, whereas the higher concentration showed no difference. Finally, the HyCaSD reaction was performed at various reaction times, ranging from 10 to 60 min (Fig. 2b). The fluorescence intensity was increased with the longer

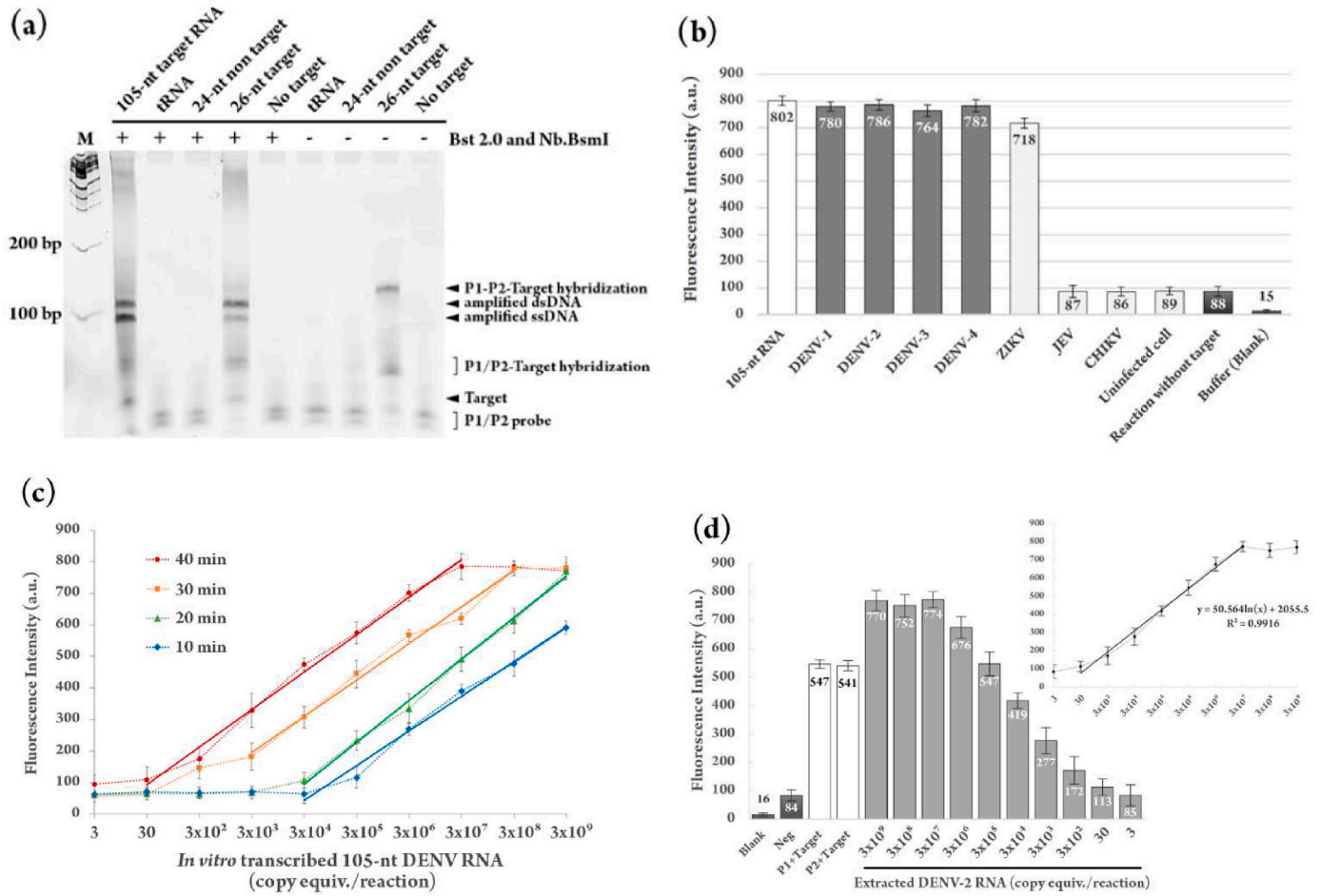

Fig. 3. Target selectivity and LOD of the MB-based HyCaSD. **(a)** The detection selectivity of the method with the *in vitro* transcribed 105-nt DENV RNA was verified. The tRNA and the 24-nt non-target DNA were used as a negative control. The 26-nt target DNA, which possessed a partial-overlapping sequence with the target sequence, was included. The result was analyzed using 10% PAGE with SYBR Gold staining; **(b)** The detection selectivity of the method with the extracted RNA of DENV1-4, ZIKV, JEV, and CHIKV. The extracted total RNA of uninfected C6/36 cell, the reaction without target RNA, and reaction buffer-only were included as a negative control; **(c** and **d)** LOD of the MB-based HyCaSD for detecting the *in vitro* transcribed 105-nt DENV RNA **(c)** and the extracted DENV-2 RNA **(d)**, were estimated with different concentrations of the target RNA, ranging from 3 to 3 × 10^9 RNA copy equivalents per reaction. *Blank* represents the reaction with buffer-only, and *Neg* represents the reaction without the target RNA. The inset shows a logarithmic plot of the fluorescence intensity versus the target concentration with a linear relationship. (For interpretation of the references to colour in this figure legend, the reader is referred to the Web version of this article.)

reaction time, and the highest intensity was measured within 40 min. Therefore, the subsequent experiments were performed at 5U/rxn of Bst 2.0 DNA polymerase and 3U/rxn of Nb.BsmI nicking endonuclease for 40 min.

3.3. Target selectivity and the detection limit of the molecular beacon-based HyCaSD

The target selectivity of the MB-based HyCaSD was tested with 50 nM of the synthetic targets (a 105-nt target RNA and a 26-nt target DNA) and 50 nM of the synthetic non-targets (a $tRNA^{SER}$ and a 24-nt non-target DNA). The 26-nt target DNA possessed 22 nucleotides that overlapped with the target sequence. The 24-nt non-target DNA was a part of 16S rRNA gene of *E. canis* (Table 1, Fig. S1). As shown in Fig. 3a, the non-target tRNA and the 24-nt non-target DNA did not show hybridization nor amplification by the DNA probes. In contrast, the 26-nt target DNA was successfully hybridized by the DNA probes to form a hybridization complex, and the amplification product was then created by the enzymes. The partially overlapping target sequence could be potentially hybridized and amplified, although the amplification kinetic was lower than the intact target sequence. The results revealed a satisfactory target selectivity to discriminate the target sequences from the non-target sequences.

The target selectivity of MB-based HyCaSD was examined using the real viruses. The extracted RNA of all DENV serotypes, of other closely related species (ZIKV and JEV), and of CHIKV (which is an unrelated species but is also transmitted by mosquito) were tested. The extracted total RNA from the uninfected C6/36 cells was included as a negative control. As shown in Fig. 3b, the method efficiently amplified the target RNA of all of the DENV serotypes and ZIKV, but not JEV, CHIKV, or the uninfected C6/36 cells. This finding could be explained by the similarity of the probe binding sites. The probe binding site could accommodate a complete match of all four DENV serotype sequences. For ZIKA, the probe binding site was identical to DENV sequence except a single-nucleotide deletion at position 11 from 5′- of the 25-nt probe binding site (Fig. S1) [12]. Taken together, a satisfactory selectivity of the MB-based HyCaSD to distinguish DENV/ZIKV from the closely related species, JEV, as well as the unrelated species, CHIKV, was achieved.

The lower detection limit of MB-based HyCaSD was determined using varied concentrations of the *in vitro* transcribed 105-nt DENV RNA, ranging from 3 to 3 × 10^9 copy equivalents per reaction, with the reaction time of 10, 20, 30, and 40 min. The linear relationship with correlation coefficient (R2) between the fluorescence intensity and the concentration of the target RNA was constructed. The LOD was

Table 2
The lower detection limit of the MB-based HyCaSD for (a) the *in vitro* transcribed 105-nt DENV RNA with varied reaction time, (b) the extracted DENV-2 RNA with 40-min reaction time.

Reaction time (minute)	Linear range (copy equivalents/reaction)	Linear regression equation[a]	Correlation coefficient (R2)	Base line signal (mean fluorescence intensity+3[a]SD)	The lower detection limit (LOD)	
					Copy equivalents/ reaction	Molar
The *in vitro* transcribed 105-nt DENV RNA with varied reaction time (a)						
10	3×10^4 to 3×10^9	y = 47.619ln(x)+ 1579.4	0.9895	127	173,000	5.7×10^{-14}
20	3×10^4 to 3×10^9	y = 57.195ln(x)+ 1939.7	0.9964	115	40,000	1.3×10^{-14}
30	3×10^3 to 3×10^8	y = 50.196ln(x)+ 1928.2	0.9892	115	600	1.9×10^{-16}
40	3×10^1 to 3×10^7	y = 51.578ln(x)+ 2112.8	0.9926	136	60	2.1×10^{-17}
The extracted DENV-2 RNA with 40-min reaction time (b)						
40	3×10^1 to 3×10^7	y = 50.564ln(x)+ 2055.5	0.9916	141	100	3.5×10^{-17}

[a] y and x represent the fluorescence intensity and the target RNA concentration, respectively.

calculated using the mean fluorescence intensity plus 3*SD (standard deviation) (Table 2). The results revealed that the target RNA could be detected at reaction time of 10 min, however the MB-based HyCaSD with longer reaction time (40 min) was able to reach the least limit of detection (60 copy equivalents per reaction). Because of the combination of the molecular beacon to HyCaSD effectively reduced non-specific amplification signal, the base line signal was very low. The LOD could achieve excellent sensitivity for detecting the *in vitro* transcribed RNA. Of note, the hybridization efficiency is a crucial factor in MB-based HyCaSD. In this study, the complicated structure of the probe binding site may affect the reaction time. Therefore, in favor of the lower LOD, the reaction time of 40 min was chosen.

The lower detection limit of the MB-based HyCaSD for the real viruses was then determined with the extracted RNA of DENV-2. The LOD for the extracted DENV-2 RNA was approximately 100 copy equivalents per reaction (~35.2 aM) (Table 2, Fig. 3d). The LOD of the extracted DENV RNA was slightly higher than the *in vitro* transcribed 105-nt DENV RNA. However, the LOD of MB-based HyCaSD method was around 20-times lower compared with the LOD of ~2000 copy equivalents per reaction of the original HyCaSD. The results indicated that the real virus was successfully detected by the MB-based HyCaSD method with an excellent sensitivity. The combination of the molecular beacon and HyCaSD method greatly enhanced the sensitivity of RNA target detection from the original HyCaSD. Although a number of isothermal amplifications have been recently established [36,37], RT-LAMP are the most popular method developed for DENV detection [38–42]. RT-LAMP has been demonstrated to be a highly sensitive isothermal amplification platform for detection of DENV. However, it has been developed only for DENV specific serotypes detection. Whereas the MB-based HyCaSD in the present study, was designed for detecting all 4 DENV serotypes in a single test. With a requirement of multiple primers (4 or 6 primers) of the LAMP, it may be difficult to find suitable sites within the complicated secondary structure of the virus 3′UTR. In comparison, the MB-based HyCaSD can be designed for each DENV serotype detection, if needed. The principle of our MB-based HyCaSD was more similar to nicking and extension amplification reaction (NEAR), another high-efficiency isothermal amplification method. Integration of molecular beacon probes into HyCaSD thus allowed single step, single tube, actual time RNA detection procedure with no requirement of reverse transcription and post-staining step.

4. Conclusion

The molecular beacon-based HyCaSD biosensor platform successfully improved the sensitivity for RNA detection, achieving an excellent sensitivity with an LOD of ~100 copy equivalents per reaction for DENV RNA detection (around 20-times lower than that of the original HyCaSD). The HyCaSD probes were labeled with the fluorophore and the quencher at each end of the hairpin probes. Therefore, like the molecular beacon probes, the fluorescence signal was detected immediately only when the DNA probes specifically hybridized to the target sequence and unfolded their hairpin structures. With this strategy, the MB-based HyCaSD eliminated the need for the post-staining step, which was a cause of high background signal and reduced sensitivity. Moreover, a single-step, single-tube, and actual-time RNA detection was enabled, which represents a major step closer to POC diagnostic applications for viral infectious diseases.

Author contributions

The manuscript was written through contributions of all authors. All authors have given approval to the final version of the manuscript.

Funding

This project received a grant from Faculty of Medicine Siriraj Hospital.

Declaration of competing interest

The authors declare that they have no known competing financial interests or personal relationships that could have appeared to influence the work reported in this paper.

Appendix A. Supplementary data

Supplementary data to this article can be found online at https://doi.org/10.1016/j.aca.2022.340134.

References

[1] X.Y. Huang, X.N. Hu, H. Ma, Y.H. Du, H.X. Ma, K. Kang, A.G. You, H.F. Wang, L. Zhang, H.M. Chen, J.S. Dumler, B.L. Xu, Detection of new bunyavirus RNA by reverse transcription-loop-mediated isothermal amplification, J. Clin. Microbiol. 52 (2) (2014) 531–535.
[2] D.C. Nyan, K.L. Swinson, A novel multiplex isothermal amplification method for rapid detection and identification of viruses, Sci. Rep. 5 (2015), 17925.
[3] H.J. Yoo, C. Baek, M.H. Lee, J. Min, Integrated microsystems for the in situ genetic detection of dengue virus in whole blood using direct sample preparation and isothermal amplification, Analyst 145 (6) (2020) 2405–2411.
[4] L. Ma, F. Zeng, B. Huang, Y. Zhu, M. Wu, F. Xu, L. Xiao, R. Huang, J. Ma, F. Cong, P. Guo, Point-of-care diagnostic assay for rapid detection of porcine deltacoronavirus using the recombinase polymerase amplification method, Transbound. Emerg. Dis. 66 (3) (2019) 1324–1331.
[5] E.K. Alidjinou, N. Lefebvre, A. Dewilde, M. Maki, D. Hober, I. Engelmann, Evaluation of the reverse transcription strand invasion based amplification (RT-SIBA) RSV assay, a rapid molecular assay for the detection of respiratory syncytial virus, Diagn. Microbiol. Infect. Dis. 95 (1) (2019) 55–58.

[6] P.F.N. Estrela, G.M. Mendes, K.G. de Oliveira, A.M. Bailao, C.M.A. Soares, N. A. Assuncao, G.R.M. Duarte, Ten-minute direct detection of Zika virus in serum samples by RT-LAMP, J. Virol. Methods 271 (2019), 113675.
[7] S.J. Ahn, Y.H. Baek, K.K.S. Lloren, W.S. Choi, J.H. Jeong, K.J.C. Antigua, H. I. Kwon, S.J. Park, E.H. Kim, Y.I. Kim, Y.J. Si, S.B. Hong, K.S. Shin, S. Chun, Y. K. Choi, M.S. Song, Rapid and simple colorimetric detection of multiple influenza viruses infecting humans using a reverse transcriptional loop-mediated isothermal amplification (RT-LAMP) diagnostic platform, BMC Infect. Dis. 19 (1) (2019) 676.
[8] K. Hayashida, Y. Orba, P.C. Sequeira, C. Sugimoto, W.W. Hall, Y. Eshita, Y. Suzuki, L. Runtuwene, P. Brasil, G. Calvet, C.D.S. Rodrigues, C.C.D. Santos, M.A.M. Mares-Guia, J. Yamagishi, A.M.B. Filippis, H. Sawa, Field diagnosis and genotyping of chikungunya virus using a dried reverse transcription loop-mediated isothermal amplification (LAMP) assay and MinION sequencing, PLoS Negl Trop Dis 13 (6) (2019), e0007480.
[9] J.Y. Lee, J.H. Kim, J.Y. Rho, Development of rapid and specific detection for the human aichivirus A using the loop-mediated isothermal amplification from water samples, Indian. J. Microbiol. 59 (3) (2019) 375–378.
[10] H. Liu, L.X. Li, Y.P. Bu, Y. Liu, X.T. Sun, N. Shi, X.Y. Deng, R.G. Lu, B. Hu, N.Y. Jin, X.J. Yan, Rapid visual detection of getah virus using a loop-mediated isothermal amplification method, Vector. Borne. Zoonotic. Dis. 19 (10) (2019) 741–746.
[11] V.L. Fowler, B. Armson, J.L. Gonzales, E.L. Wise, E.L.A. Howson, Z. Vincent-Mistiaen, S. Fouch, C.J. Maltby, S. Grippon, S. Munro, L. Jones, T. Holmes, C. Tillyer, J. Elwell, A. Sowood, O. de Peyer, S. Dixon, T. Hatcher, H. Patrick, S. Laxman, C. Walsh, M. Andreou, N. Morant, D. Clark, N. Moore, R. Houghton, N. J. Cortes, S.P. Kidd, A highly effective reverse-transcription loop-mediated isothermal amplification (RT-LAMP) assay for the rapid detection of SARS-CoV-2 infection, J. Infect. 82 (1) (2021) 117–125.
[12] W. Saisuk, C. Srisawat, S. Yoksan, T. Dharakul, Hybridization cascade plus strand-displacement isothermal amplification of RNA target with secondary structure motifs and its application for detecting dengue and Zika viruses, Anal. Chem. 91 (5) (2019) 3286–3293.
[13] O.A. Sonmezoglu, K. Ozkay, A new organic dye-based staining for the detection of plant DNA in agarose gels, Nucleos. Nucleot. Nucl. 34 (7) (2015) 515–522.
[14] Q. Huang, W.L. Fu, Comparative analysis of the DNA staining efficiencies of different fluorescent dyes in preparative agarose gel electrophoresis, Clin. Chem. Lab. Med. 43 (8) (2005) 841–842.
[15] T. Ohta, S. Tokishita, H. Yamagata, Ethidium bromide and SYBR Green I enhance the genotoxicity of UV-irradiation and chemical mutagens in E. coli, Mutat. Res. 492 (1–2) (2001) 91–97.
[16] S. Phukan, S. Mitra, Fluorescence behavior of ethidium bromide in homogeneous solvents and in presence of bile acid hosts, J. Photochem. Photobiol. A 244 (2012) 9–17.
[17] S. Nafisi, A.A. Saboury, N. Keramat, J.F. Neault, H.A. Tajmir-Riahi, Stability and structural features of DNA intercalation with ethidium bromide, acridine orange and methylene blue, J. Mol. Struct. 827 (1) (2007) 35–43.
[18] A.I. Dragan, R. Pavlovic, J.B. McGivney, J.R. Casas-Finet, E.S. Bishop, R.J. Strouse, M.A. Schenerman, C.D. Geddes, SYBR green I: fluorescence properties and interaction with DNA, J. Fluoresc. 22 (4) (2012) 1189–1199.
[19] V.L. Singer, T.E. Lawlor, S. Yue, Comparison of SYBR® Green I nucleic acid gel stain mutagenicity and ethidium bromide mutagenicity in the Salmonella/mammalian microsome reverse mutation assay (Ames test), Mutat. Res. Genet. Toxicol. Environ. Mutagen. 439 (1) (1999) 37–47.
[20] S. Nafisi, A.A. Saboury, N. Keramat, J.-F. Neault, H.-A. Tajmir-Riahi, Stability and structural features of DNA intercalation with ethidium bromide, acridine orange and methylene blue, J. Mol. Struct. 827 (1) (2007) 35–43.
[21] J.N. Zadeh, C.D. Steenberg, J.S. Bois, B.R. Wolfe, M.B. Pierce, A.R. Khan, R. M. Dirks, N.A. Pierce, NUPACK: analysis and design of nucleic acid systems, J. Comput. Chem. 32 (1) (2011) 170–173.
[22] N.G. Iglesias, A.V. Gamarnik, Dynamic RNA structures in the dengue virus genome, RNA Biol 8 (2) (2011) 249–257.
[23] E. Southern, K. Mir, M. Shchepinov, Molecular interactions on microarrays, Nat. Genet. 21 (1 Suppl) (1999) 5–9.
[24] S. Lane, J. Evermann, F. Loge, D.R. Call, Amplicon secondary structure prevents target hybridization to oligonucleotide microarrays, Biosens. Bioelectron. 20 (4) (2004) 728–735.
[25] W.F. Lima, B.P. Monia, D.J. Ecker, S.M. Freier, Implication of RNA structure on antisense oligonucleotide hybridization kinetics, Biochemistry 31 (48) (1992) 12055–12061.
[26] A. Tsourkas, M.A. Behlke, S.D. Rose, G. Bao, Hybridization kinetics and thermodynamics of molecular beacons, Nucleic Acids Res 31 (4) (2003) 1319–1330.
[27] W. Liu, S. Huang, N. Liu, D. Dong, Z. Yang, Y. Tang, W. Ma, X. He, D. Ao, Y. Xu, D. Zou, L. Huang, Establishment of an accurate and fast detection method using molecular beacons in loop-mediated isothermal amplification assay, Sci. Rep. 7 (2017), 40125.
[28] J.A. Vet, A.R. Majithia, S.A. Marras, S. Tyagi, S. Dube, B.J. Poiesz, F.R. Kramer, Multiplex detection of four pathogenic retroviruses using molecular beacons, Proc. Natl. Acad. Sci. U.S.A. 96 (11) (1999) 6394–6399.
[29] C. Nguyen, J. Grimes, Y.V. Gerasimova, D.M. Kolpashchikov, Molecular-beacon-based tricomponent probe for SNP analysis in folded nucleic acids, Chemistry (Weinheim an der Bergstrasse, Germany) 17 (46) (2011) 13052–13058.
[30] Y. Gao, L.K. Wolf, R.M. Georgiadis, Secondary structure effects on DNA hybridization kinetics: a solution versus surface comparison, Nucleic Acids Res 34 (11) (2006) 3370–3377.
[31] C. Chen, W. Wang, Z. Wang, F. Wei, X.S. Zhao, Influence of secondary structure on kinetics and reaction mechanism of DNA hybridization, Nucleic Acids Res 35 (9) (2007) 2875–2884.
[32] J.R. Grunwell, J.L. Glass, T.D. Lacoste, A.A. Deniz, D.S. Chemla, P.G. Schultz, Monitoring the conformational fluctuations of DNA hairpins using single-pair fluorescence resonance energy transfer, J. Am. Chem. Soc. 123 (18) (2001) 4295–4303.
[33] M.T. Woodside, W.M. Behnke-Parks, K. Larizadeh, K. Travers, D. Herschlag, S. M. Block, Nanomechanical measurements of the sequence-dependent folding landscapes of single nucleic acid hairpins, Proc. Natl. Acad. Sci. U.S.A. 103 (16) (2006) 6190–6195.
[34] R. Narayanan, L. Zhu, Y. Velmurugu, J. Roca, S.V. Kuznetsov, G. Prehna, L. J. Lapidus, A. Ansari, Exploring the energy landscape of nucleic acid hairpins using laser temperature-jump and microfluidic mixing, J. Am. Chem. Soc. 134 (46) (2012) 18952–18963.
[35] L. Ying, M.I. Wallace, D. Klenerman, Two-state model of conformational fluctuation in a DNA hairpin-loop, Chem. Phys. Lett. 334 (1) (2001) 145–150.
[36] Y. Zhang, G. Ren, J. Buss, A.J. Barry, G.C. Patton, N.A. Tanner, Enhancing colorimetric loop-mediated isothermal amplification speed and sensitivity with guanidine chloride, Biotechniques 69 (3) (2020) 178–185.
[37] J. Zhao, S. Fang, Y. Liu, L. Zeng, Z. He, A lateral flow biosensor based on gold nanoparticles detects four hemorrhagic fever viruses, Anal. Methods. 12 (2020) 5613–5620.
[38] P.C. Sigera, R. Amarasekara, C. Rodrigo, S. Rajapakse, P. Weeratunga, N.L. De Silva, C.H. Huang, M.K. Sahoo, B.A. Pinsky, D.R. Pillai, H.A. Tissera, S. Jayasinghe, S. Handunnetti, S.D. Fernando, Risk prediction for severe disease and better diagnostic accuracy in early dengue infection; the Colombo dengue study, BMC Infect Dis 19 (1) (2019) 680.
[39] B.T. Teoh, S.S. Sam, K.K. Tan, J. Johari, M.B. Danlami, P.S. Hooi, R. Md-Esa, S. AbuBakar, Detection of dengue viruses using reverse transcription-loop-mediated isothermal amplification, BMC Infect Dis 21 (13) (2013) 387.
[40] J. Kim, S.H. Baek, S. Kim, H.I. Kim, S.W. Lee, L. Tu Phan, S.K. Kailasa, T.J. Park, Rapid discriminative detection of dengue viruses via loop mediated isothermal amplification, Talanta 190 (2018) 391–396.
[41] B. Huang, B.L. Montgomery, R. Adamczyk, G. Ehlers, A.F. van den Hurk, D. Warrilow, A LAMP-based colorimetric assay to expedite field surveillance of the invasive mosquito species Aedes aegypti and Aedes albopictus, PLoS Negl. Trop. Dis. 14 (3) (2020).
[42] S. Kumar, S. Sharma, N. Bhardwaj, V. Pande, D. Savargaonkar, A.R. Anvikar, Advanced Lyophilised Loop Mediated Isothermal Amplification (L-LAMP) based point of care technique for the detection of dengue virus, J. Virol. Methods. 293 (2021), 114168.